Parathyroid Hormone-related Peptide-depleted Mice Show Abnormal Epiphyseal Cartilage Development and Altered Endochondral Bone Formation

Norio Amizuka,*‖ Hershey Warshawsky,‡ Janet E. Henderson,*¶ David Goltzman,*§‖ and Andrew C. Karaplis*¶

*Department of Medicine, ‡Anatomy and Cell Biology, and §Physiology, McGill University, Montréal, Québec, Canada H3A 2T5; and ‖Calcium Research Laboratory, Royal Victoria Hospital, Montréal, Québec, Canada H3A 1A1; and ¶Endocrine Division, Sir Mortimer B. Davis-Jewish General Hospital, Lady Davis Institute for Medical Research, Montréal, Québec, Canada H3T 1E2

Abstract. To elucidate the role of PTHrP in skeletal development, we examined the proximal tibial epiphysis and metaphysis of wild-type (PTHrP-normal) 18–19-d-old fetal mice and of chondrodystrophic litter mates homozygous for a disrupted PTHrP allele generated via homologous recombination in embryonic stem cells (PTHrP-depleted). In the PTHrP-normal epiphysis, immunocytochemistry showed PTHrP to be localized in chondrocytes within the resting zone and at the junction between proliferative and hypertrophic zones. In PTHrP-depleted epiphyses, a diminished [^{3}H]thymidine-labeling index was observed in the resting and proliferative zones accounting for reduced numbers of epiphyseal chondrocytes and for a thinner epiphyseal plate. In the mutant hypertrophic zone, enlarged chondrocytes were interspersed with clusters of cells that did not hypertrophy, but resembled resting or proliferative chondrocytes. Although the overall content of type II collagen in the epiphyseal plate was diminished, the lacunae of these non-hypertrophic chondrocytes did react for type II collagen. Moreover, cell membrane–associated chondroitin sulfate immunoreactivity was evident on these cells. Despite the presence of alkaline phosphatase activity on these non-hypertrophic chondrocytes, the adjacent cartilage matrix did not calcify and their persistence accounted for distorted chondrocyte columns and sporadic distribution of calcified cartilage. Consequently, in the metaphysis, bone deposited on the irregular and sparse scaffold of calcified cartilage and resulted in mixed spicules that did not parallel the longitudinal axis of the tibia and were, therefore, inappropriate for bone elongation. Thus, PTHrP appears to modulate both the proliferation and differentiation of chondrocytes and its absence alters the temporal and spatial sequence of epiphyseal cartilage development and of subsequent endochondral bone formation necessary for normal elongation of long bones.

PARATHYROID hormone–related peptide (PTHrP)[1] was originally identified as a pathogenetic factor for malignancy-associated hypercalcemia (Suva et al., 1987; Burtis et al., 1987; Strewler et al., 1987). The homology of the NH_2-terminal region of PTHrP with the corresponding domain of parathyroid hormone (PTH), and the resultant capacity of both molecules to interact with a common receptor (Jüppner et al., 1991) appear to account for the ability of PTHrP to mimic many of the effects of PTH on calcium and phosphate homeostasis and on skeletal turnover (Rodan et al., 1983; Horiuchi et al., 1987; Kemp et al., 1987; Rabbani et al., 1988). Unlike PTH, however, whose synthesis is restricted to the parathyroid gland, PTHrP is produced in diverse normal adult (Merendino et al., 1986; Thiede et al., 1988; Kramer et al., 1991) and fetal (Senior et al., 1991) tissues, suggesting that it may play a broader role than simply as a hypercalcemia-inducing oncoprotein. Indeed, in vitro studies employing antisense technology (Kaiser et al., 1992, 1994) and transgenic studies overexpressing PTHrP in mice (Wysolmerski et al., 1994) have implicated a role for PTHrP in modulation of cell growth and differentiation. In embryogenesis, it has been suggested that PTHrP acts as an endogenous inducer of parietal endoderm differentiation (Stolpe et al., 1993). Nevertheless, little is known of the definitive role of PTHrP in the development and function of the organism in vivo.

Address all correspondence to Dr. Andrew C. Karaplis, Lady Davis Institute for Medical Research, Room 626, 3755 Côte-Ste-Catherine Road, Montréal, Québec, Canada H3T 1E2. Telephone: (514) 340-8260; FAX: (514) 340-7573.

The current address of Norio Amizuka is Niigata University School of Dentistry, 1st Department of Oral Anatomy, Niigata, Japan.

1. *Abbreviations used in this paper*: ALPase, alkaline phosphatase; ES, embryonic stem; PTH, parathyroid hormone; PTHrP, parathyroid hormone-related peptide; TRACPase, tartrate-resistant acid phosphatase.

Recently, the PTHrP gene has been inactivated in mice using gene targeting by homologous recombination in embryonic stem (ES) cells (Karaplis et al., 1994). Mice lacking PTHrP die immediately after birth, possibly due to respiratory compromise as a consequence of marked thoracic wall deformities. Skeletal abnormalities are widespread, however, suggesting a fundamental defect in endochondral bone formation. The present study was therefore undertaken to examine cartilage and endochondral bone development in the PTHrP-depleted (homozygous) mice as compared to the PTHrP-normal (wild-type) litter mates.

Materials and Methods

PTHrP-depleted Mice

Mice carrying a disrupted, nonfunctional PTHrP gene were derived by homologous recombination in an ES cell line of 129/Sv genetic background as previously described (Karaplis et al., 1994). To analyze endochondral bone formation, mice heterozygous for the PTHrP gene ablation were mated and fetuses were delivered by caesarean section 18–19 d *post coitum*. PTHrP-normal and homozygous litter mates were genotypes using Southern blot analysis of tail genomic DNA (Karaplis et al., 1994). Tibiae from these animals were dissected under a binocular microscope and the proximal epiphyses were processed for histological, radioautographic, cytochemical, and immunocytochemical analyses.

Tissue Preparation, Fixation, and Embedding

For transmission electron microscopy and for radioautography, the tibiae were immersed in a mixture of 2% paraformaldehyde and 2.5% glutaraldehyde in 0.1 M phosphate buffer (pH 7.4). For enzyme cytochemistry and immunocytochemistry, tibiae were immersed in 4% paraformaldehyde in 0.1 M cacodylate buffer (pH 7.4). Most specimens were then decalcified with 4.13% EDTA (pH 7.4) at 4°C for 48 h (Warshawsky and Moore, 1967). For ultrastructure and radioautography, specimens were postfixed in an aqueous solution of 1% OsO_4 and 1.5% ferrocyanide at 4°C for 2 h, dehydrated in a graded series of acetone and embedded in Epon 812. Some specimens fixed with paraformaldehyde were dehydrated in a graded ethanol series and embedded in either paraffin or Technovit 7100 (Kulzer, Germany), some were frozen immediately by immersion in liquid nitrogen, and others were dehydrated in N,N-dimethylformamide and embedded in glycolmethacrylate before UV polymerization. Observations were made with a JEOL 2000FX electron microscope operated at 80 kV.

Radioautography

To estimate cell proliferation, an aqueous solution of [^{3}H]thymidine (1 μCi/g body weight; specific activity 1 μCi/μl, NEN Research Products, Canada) was injected into the external jugular vein of pregnant, heterozygous female mice at 18–19 d into gestation. To assess the overall protein synthetic rate, an aqueous solution of [^{3}H]proline (30 μCi/g body weight; specific activity 1 μCi/μl, NEN Research Products) was similarly injected. After 4 h in each case, fetuses were delivered by cesarean section and the fetal tibiae were removed and embedded in Epon 812 as described above. Longitudinal 1-μm thick sections of tibiae were mounted on glass slides and stained with iron hematoxylin before dipping in Kodak NTB-2 liquid emulsion for radioautography. Sections of tissues labeled with [^{3}H]thymidine or [^{3}H]proline were exposed at 4°C for 2 mo or 2 wk, respectively.

For quantitative analysis of DNA synthesis, the total number of chondrocytes and chondrocytes labeled with [^{3}H]thymidine were counted in the resting, proliferative, and hypertrophic zones of the epiphyseal cartilage. In bone tissue, all cells except bone marrow cells and all cells labeled with silver grains were counted in a 2,500 μm^2 area under a Whipple micrometer ocular grid (Wild, Switzerland) at a magnification of ×640. An index of DNA synthesis ([^{3}H]thymidine-labeling index) was obtained, in each case, by dividing the number of cells labeled with grains by the total number of cells and expressed as a percentage.

Similarly, for quantitative assessment of protein synthetic activity in the epiphyseal cartilage, as assessed by [^{3}H]proline labeling, all silver grains over matching regions of chondrocytes and cartilage matrix were counted and divided by the number of chondrocytes in that region. In bone tissue, silver grains were counted over individual osteoblasts and the adjacent bone matrix and expressed as the number of grains per osteoblast.

Student's *t* test for statistical significance of the mean was employed to analyze all counts.

Cytochemistry

Alkaline phosphatase. Alkaline phosphatase (ALPase) activity was detected by the method of Oguro and Ozawa (1989). In brief, 20–40-μm frozen

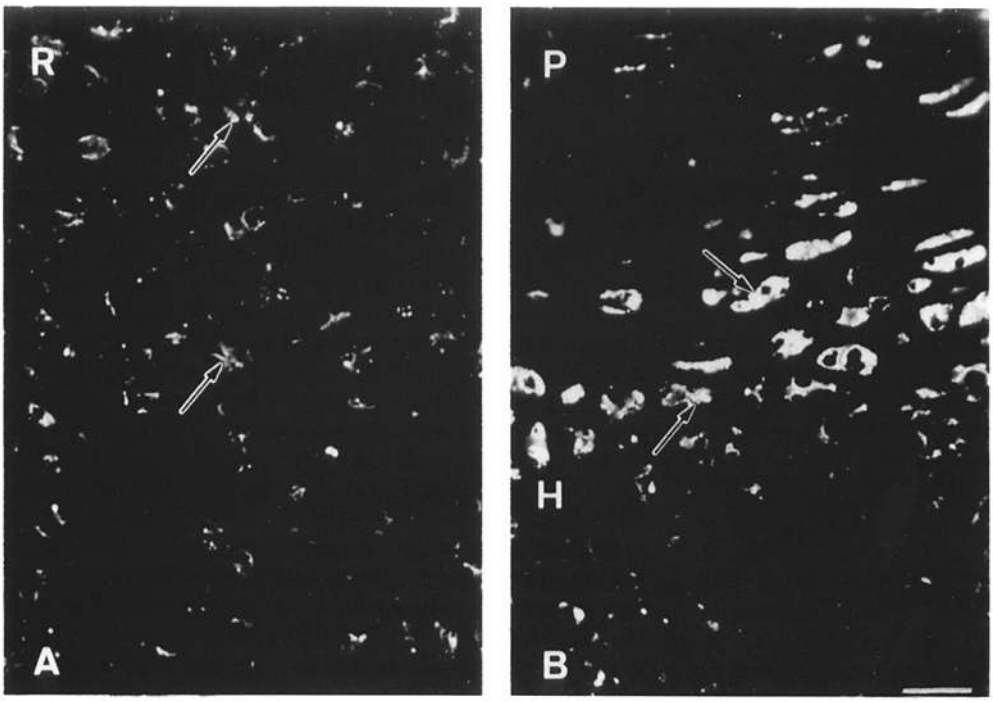

Figure 1. Confocal laser micrographs of PTHrP immunoreactivity in chondrocytes of the proximal tibial epiphyses of 18–19-d old PTHrP-normal fetuses. PTHrP immunoreactivity (*arrows*) is observed in the cytoplasm of chondrocytes in the resting zone (*R* in *A*) and in transitional chondrocytes at the junction between proliferative (*P*) and hypertrophic (*H*) zones (*B*). Hypertrophic chondrocytes display no PTHrP immunoreactivity. Immunofluorescence was performed as described in Materials and Methods. No reaction was observed when the primary antiserum was omitted, when the primary antiserum was preincubated with excess PTHrP (1-34), or when immunofluorescence was performed on the tibial epiphyses of PTHrP-depleted mice. Bar: (*A* and *B*) 15 μm.

sections were preincubated in an aqueous solution of 50 mM $MgSO_4$ in 0.1 M Tris-maleate buffer (pH 7.4) at room temperature for 60 min, and then incubated in a mixture of 8.4% sucrose, 0.74% β-glycerophosphate, 0.19% $MgSO_4$ and 0.24% lead citrate in 0.1 M Tris-HCl buffer (pH 8.5) for 30–60 min at 37°C. Specimens were then embedded in Technovit 7100, sectioned at a thickness of 1 μm and treated with dilute ammonium sulfide for visualization of the ALPase reaction.

Tartrate-resistant acid phosphatase. For detection of tartrate-resistant acid phosphatase (TRACPase) activity according to Burstone (1958), longitudinal Technovit sections of 1–2 μm thickness were collected on poly L-lysine–coated glass slides (Polyscience Inc., Warrington, PA), and then incubated for 30 min at 37°C in an aqueous solution of 0.008% naphthol AS-TR phosphate (Sigma Chemical Co., St. Louis, MO), 0.07% red violet LB salt (Sigma) and 0.76% L(+)-tartaric acid (50 mM; Sigma) in 0.1 M sodium acetate buffer (pH 5.0). TRACPase-positive cells were then counted in whole sections of the tibiae. Cells with more than two nuclei were regarded as osteoclasts. The means were analyzed with the Student's *t* test for significance.

Immunocytochemistry

PTHrP detection. Paraffin sections collected on poly-L-lysine–coated glass slides were preincubated in PBS (pH 7.4) with 2% BSA-PBS for 30 min at room temperature. Sections were then incubated with rabbit antiserum against PTHrP (1-34) (Henderson et al., 1990) at a dilution of 1:200–300 for 18 h at 4°C. After rinsing with PBS, sections were incubated with FITC-conjugated mouse anti-rabbit IgG (Dakopotts, Denmark) at a dilution of 1:100 for 18 h at 4°C. Immunofluorescence was examined using a confocal laser microscope (Olympus LSM-GB 200, Japan).

Type II collagen detection. Longitudinal frozen sections of 50 μm thickness, with or without hyaluronidase pretreatment, were incubated in 1% BSA-PBS for 30 min, and then for 18 h at 4°C in medium containing mono-

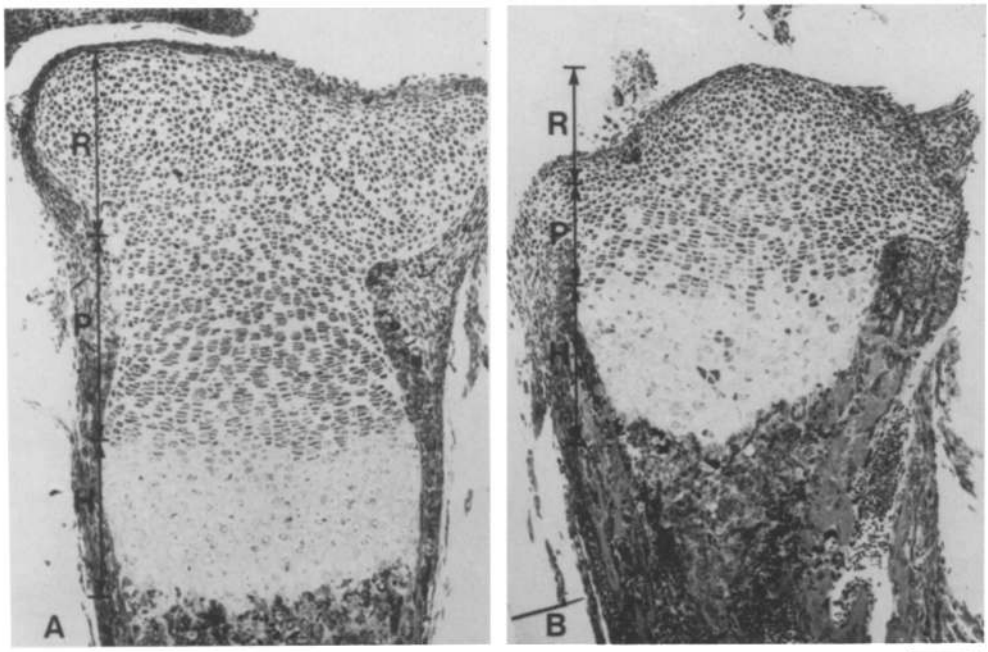

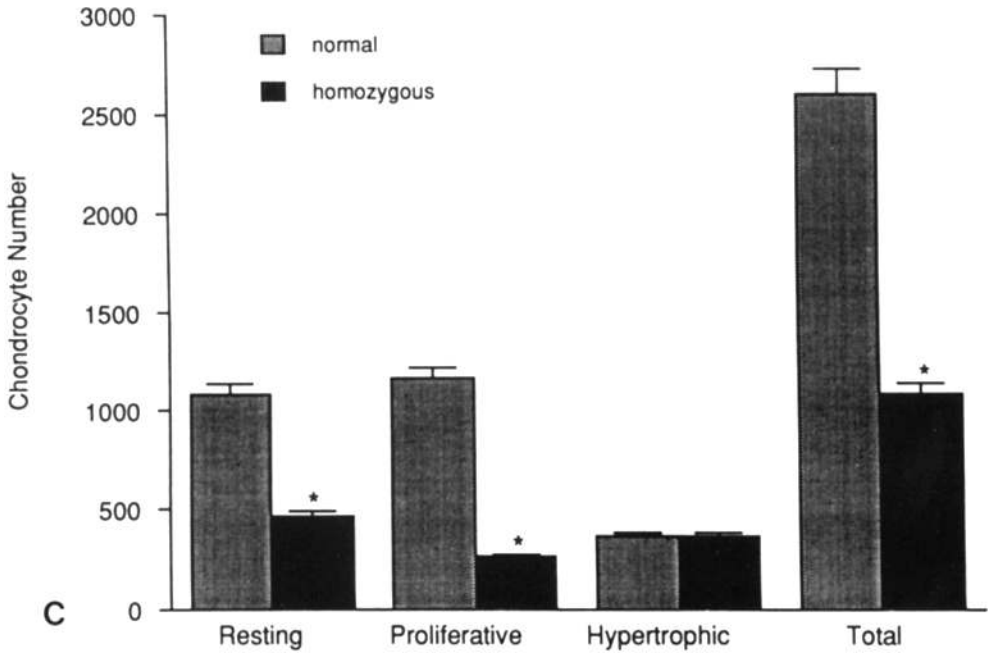

Figure 2. Low magnification photomicrographs of the proximal tibiae of PTHrP-normal (*A*) and PTHrP-depleted (*B*) fetal mice. (*A*) The epiphyseal cartilage of the PTHrP-normal tibia consists of distinct zones of resting (*R*), proliferative (*P*), and hypertrophic (*H*) chondrocytes, with a narrow, indistinct transitional zone between proliferation and hypertrophy. (*B*) The tibial epiphysis of PTHrP-depleted mice is shortened, both resting and proliferative zones being markedly reduced. In *C*, the numbers of resting, proliferative, and hypertrophic chondrocytes of the tibiae of PTHrP-normal and PTHrP-depleted mice are compared. Each bar represents main ± SEM (n = 10). * indicates significant difference at $p < 0.001$. Bar: (*A* and *B*) 60 μm.

clonal antibody to type II collagen (Hybridoma Bank, University of Iowa, Iowa City, IA). Specimens were subsequently incubated with FITC-conjugated goat anti-mouse IgG (Chemicon International Inc., Temecula, CA) at a 1:100 dilution for 18 h at 4°C. Immunofluorescence was visualized using confocal laser microscopy.

Proteoglycan detection. Monoclonal antibodies 2-B-6, 7-D-4 (ICN Biomedicals Inc., Costa Mesa, CA) and CS-56 (Sigma) were used for the immunocytochemical localization of glycosaminoglycans in normal and mutant tibial growth plates. Antibody 2-B-6 recognizes 4-sulfated *N*-acetylgalactosamine produced by chondroitinase ABC digestion of native chondroitin sulfate (Byers et al., 1992). Immunostaining was performed on longitudinal paraffin sections after digestion with 0.05 U/ml chondroitinase ABC (ICN) in 0.1 M Tris-acetate buffer (pH 7.4) for 90 min at 37°C. The sections were blocked with 1% BSA-PBS for 15 min at room temperature and incubated with 2-B-6 (1:100) for 60 min. Staining with 7-D-4 (epitope within native chondroitin sulfate chains; 1:50) and with CS-56 (recognizes cell-membrane associated chondroitin-sulfate; 1:100) was similarly performed except for omission of chondroitinase treatment (Byers et al., 1992; Avnur and Geiger, 1984).

All specimens were reacted with horseradish peroxidase-conjugated goat anti-mouse immunoglobulins (Calbiochem-Novabiochem Corp., La Jolla, CA) at 1:100 dilution and visualized using diaminobenzidine substrate.

Osteocalcin detection. One μm thick GMA embedded sections of tibiae were preincubated with 1% BSA-PBS for 15 min at room temperature and incubated with goat antibody to rat osteocalcin (Biomedical Technologies, Inc., Stoughton, MA) at a 1:100 dilution for 18 h at 4°C. After rinsing with PBS, specimens were incubated with rabbit anti-goat IgG (Bio-Rad Laboratories, Hercules, CA) at a dilution of 1:100 and subsequently with protein A-gold complex (Polyscience Inc., Niles, IL) at a dilution of 1:30 in 1% BSA-PBS for 1 h at room temperature. For silver enhancement (Slot and Geuze, 1985; Amizuka and Ozawa, 1992), immunogold-labeled GMA sections were incubated in a mixture of 8.5 g hydroquinone, 0.06 g maleic acid, 0.11 g silver nitrate and 10 g acacia in 0.05 M citrate buffer (pH 3.5-4.0) at room temperature in the dark until immunoreactivity was visible as a dark brown color. Sections were then lightly counterstained with toluidine blue.

Results

Localization of PTHrP in Normal Fetal Tibiae

In the tibial epiphyses of 18–19-d old wild-type fetuses, PTHrP-immunopositive chondrocytes were observed in the resting zone (Fig. 1 *A*) and in the thin zone of transition between proliferative and hypertrophic zones (Fig. 1 *B*). Immunoreactive chondrocytes were occasionally seen in the proliferative zone, but were not found in the hypertrophic zone nor in the articular or subarticular regions at the head of the tibia.

In the diaphyses, PTHrP immunoreaction was also very prominent in osteoblasts located on mixed spicules (data not shown). However, osteoclasts and endothelial cells did not display distinct immunopositivity. PTHrP immunoreactivity on sections from tibiae of PTHrP-depleted, homozygous mice was always negative.

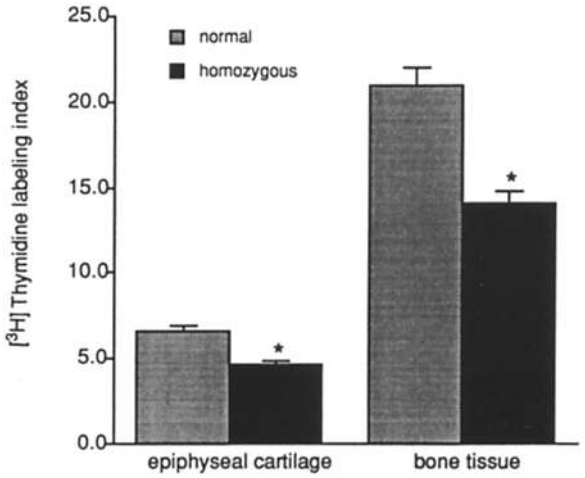

Figure 3. Percentage of [^{3}H]Thymidine-labeled cells ([^{3}H]thymidine-labeling index) in the epiphyseal cartilage and metaphyseal bone tissue of the tibiae of PTHrP-normal and PTHrP-depleted mice. [^{3}H]Thymidine-labeling index was determined in each region as described in Materials and Methods; bars represent the mean ± SEM (n = 11). * indicates significant difference at $p < 0.001$.

Alterations in the Epiphyseal Cartilage in PTHrP-depleted Mice

In mice homozygous for PTHrP gene ablation, the epiphyseal cartilage was markedly reduced in thickness (Fig. 2 *B* compared to 2 *A*). The decreased thickness of the epiphysis was due predominantly to a reduction in the number of resting and proliferative chondrocytes (Fig. 2 *C*). The [^{3}H]thymidine-labeling index was reduced in the epiphyseal chondrocytes and bone cells of the PTHrP-depleted mice (Fig. 3). Moreover, proliferative chondrocytes were not only reduced in number but did not flatten nor form typical longitudinal columns (Fig. 4 *B* compared to 4 *A*).

In the hypertrophic zone of PTHrP-normal mice, all chondrocytes became enlarged (Fig. 4 *A*). However, in PTHrP-depleted mice, clusters of non-hypertrophic chondrocytes persisted among the cells in the hypertrophic zone (Fig. 4 *B*). In the mutant specimen, the transition zone from proliferative to hypertrophic began at various levels with no clear junction in between. Furthermore, the persistence of clusters of non-hypertrophic chondrocytes up to the metaphyseal side of the epiphyseal plate distorted the longitudinal columns of hypertrophic chondrocytes resulting in the absence of longitudinal septae of cartilage matrix.

After injection of [^{3}H]thymidine, the non-hypertrophic chondrocytes in the hypertrophic zone of PTHrP-depleted mice showed numerous silver grains over the nuclei (Fig. 4 *C*) indicating DNA synthesis and thus, proliferation. No nuclear labeling was observed in hypertrophic chondrocytes of either wild type or mutant mice. Furthermore, [^{3}H]proline radioautography indicated that these non-hypertrophic chondrocytes synthesized protein more actively than hypertrophic cells (Fig. 4 *D*), although the overall amount of protein synthesis by epiphyseal chondrocytes was similar in the PTHrP-normal and PTHrP-depleted mice (data not shown). On the other hand, the non-hypertrophic chondrocytes were found to exhibit intense ALPase activity on the cell membrane (Fig. 4 *E*) identical to that of hypertrophic chondrocytes. Ultrastructurally, non-hypertrophic chondrocytes resembled chondrocytes in the resting and proliferative zones in that

Table I. Quantification of TRACPase-Positive Cells

	Multinucleated	Mononuclear
PTHrP-normal	34.3 ± 1.4	12.2 ± 0.8
PTHrP-depleted	45.5 ± 1.5*	13.5 ± 0.7

TRACPase-positive cells were counted in entire longitudinal sections of tibiae of PTHrP-normal and PTHrP-depleted mice as described in Materials and Methods. Values represent the mean ± SEM (n = 26).
* Significant at $p < 0.001$.

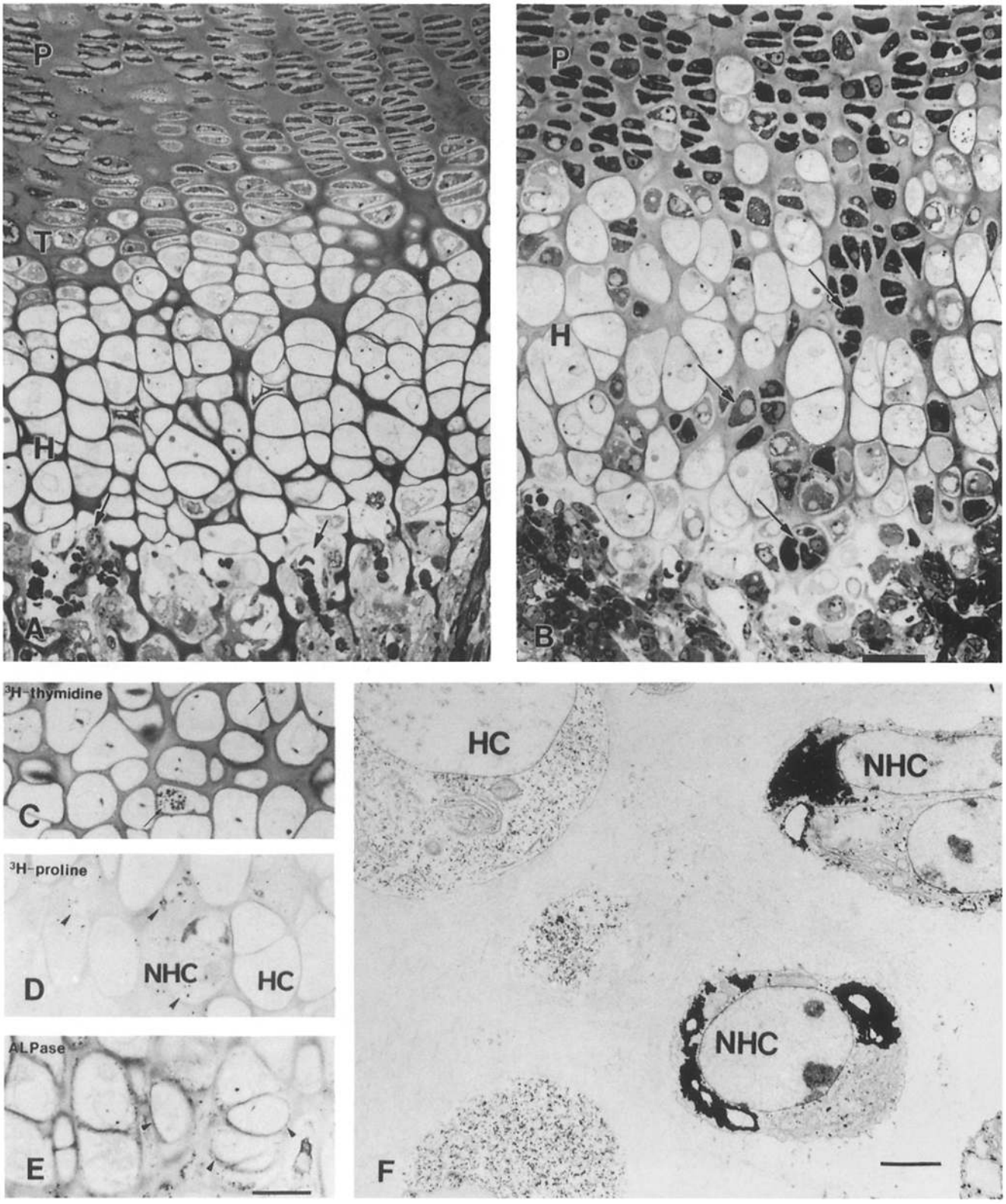

Figure 4. Photomicrographs of the tibial epiphyseal cartilage from PTHrP-normal (*A*) and PTHrP-depleted (*B*) mice, and radioautographic (*C* and *D*), cytochemical (*E*), and ultrastructural (*F*) analyses of non-hypertrophic chondrocytes (NHC) from PTHrP-depleted mice. (*A*) The normal epiphysis shows distinct proliferative (*P*), transitional (*T*), and hypertrophic (*H*) zones and longitudinal columns of both proliferative and hypertrophic chondrocytes (HC). In the zone of vascular invasion, blood vessels are seen invading empty lacunae (*arrows*). (*B*) In the epiphyses of PTHrP-depleted mice, NHC (*arrows*) are observed in clusters among the HC disrupting the formation of longitudinal columns. Numerous cells accumulate at the zone of vascular invasion and few vacant lacunae are seen here. (*C*) Light microscope radioautograph demonstrating silver grains (*arrows*) over the nuclei of NHC at 4 h after injection of [^{3}H]thymidine. (*D*) Light microscope radioautograph showing the distribution of silver grains (*arrowheads*) over NHC but not over HC after injection of [^{3}H]proline. (*E*) Photomicrograph showing the intense black reaction of ALPase (*arrowheads*) over the cell surface of NHC as well as HC. (*F*) Electron micrograph of the tibial epiphyseal hypertrophic zone of PTHrP-depleted mice demonstrates NHC containing massive cytoplasmic accumulations of electron dense glycogen granules, distended cisternae of rough endoplasmic reticulum, scattered mitochondria, and vesicles. In HC, numerous glycogen granules are dispersed throughout the cytoplasm. Bars: (*A* and *B*) 25 μm; (*C*, *D*, and *E*) 22 μm; (*F*) 4 μm.

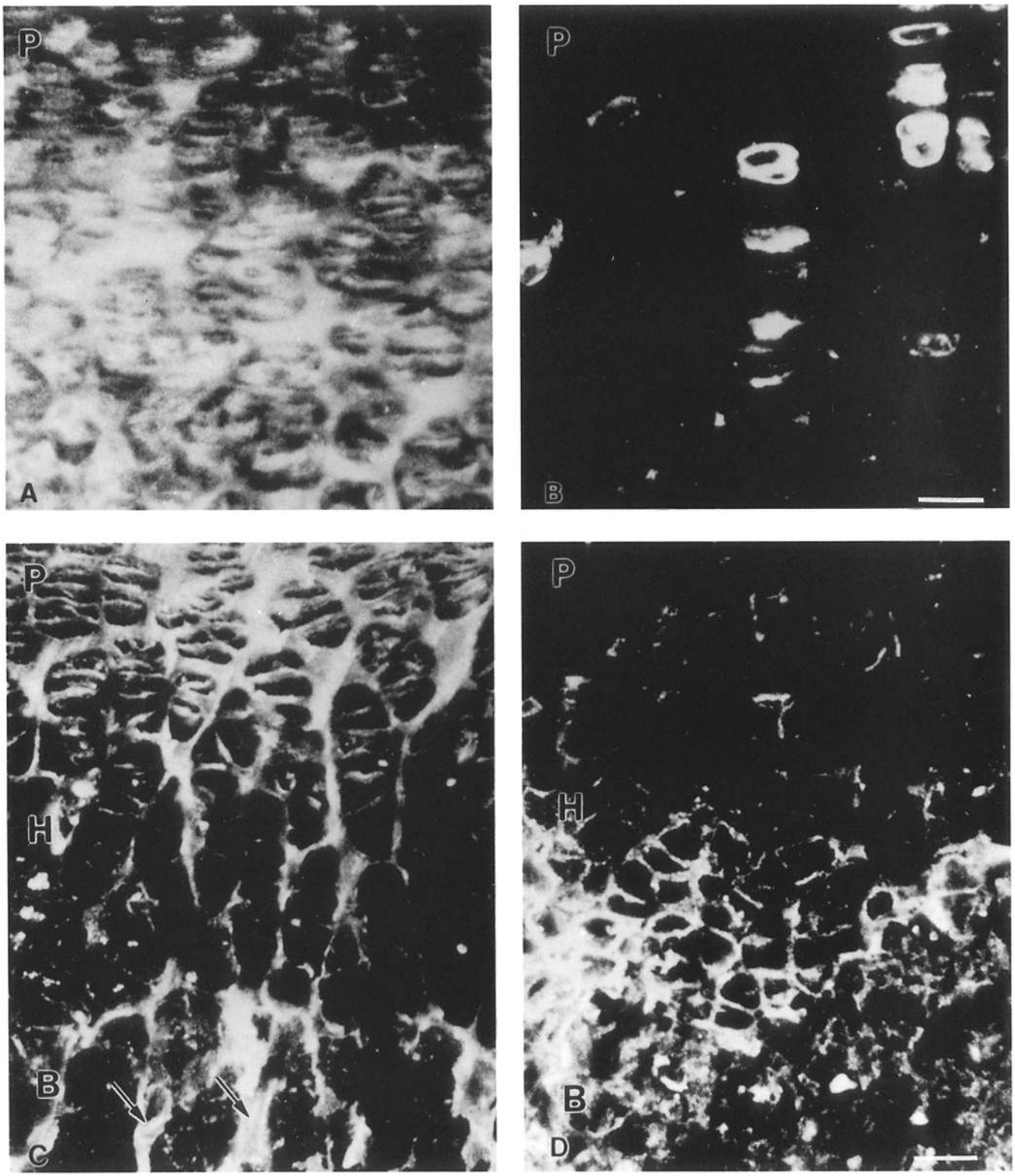

Figure 5. Confocal laser micrographs of type II collagen immunoreactivity in the tibial epiphyses of PTHrP-normal (*A* and *C*) and PTHrP-depleted (*B* and *D*) animals. (*A*) The proliferative zone (*P*) of the PTHrP-normal tibia displays bright, uniform, immunoreactivity throughout the cartilage matrix. (*B*) The proliferative zone of tibia from the homozygous mouse displays only a few immunopositive cells and a largely negative matrix. (*C*) In the hypertrophic zone (*H*) of the PTHrP-normal tibia, intense immunoreactivity is observed throughout the cartilage matrix. In the metaphyseal bone tissue (*B*), the cartilage cores of mixed spicules also display bright immunoreactivity (*arrows*). (*D*) In the hypertrophic zone of tibia from the PTHrP-depleted mouse, immunoreactivity is observed mainly in the cartilage matrix between NHC in a compact region close to bone. No immunoreactivity was observed when the primary antibody was omitted. Bars: (*A* and *B*) 15 μm; (*C* and *D*) 30 μm.

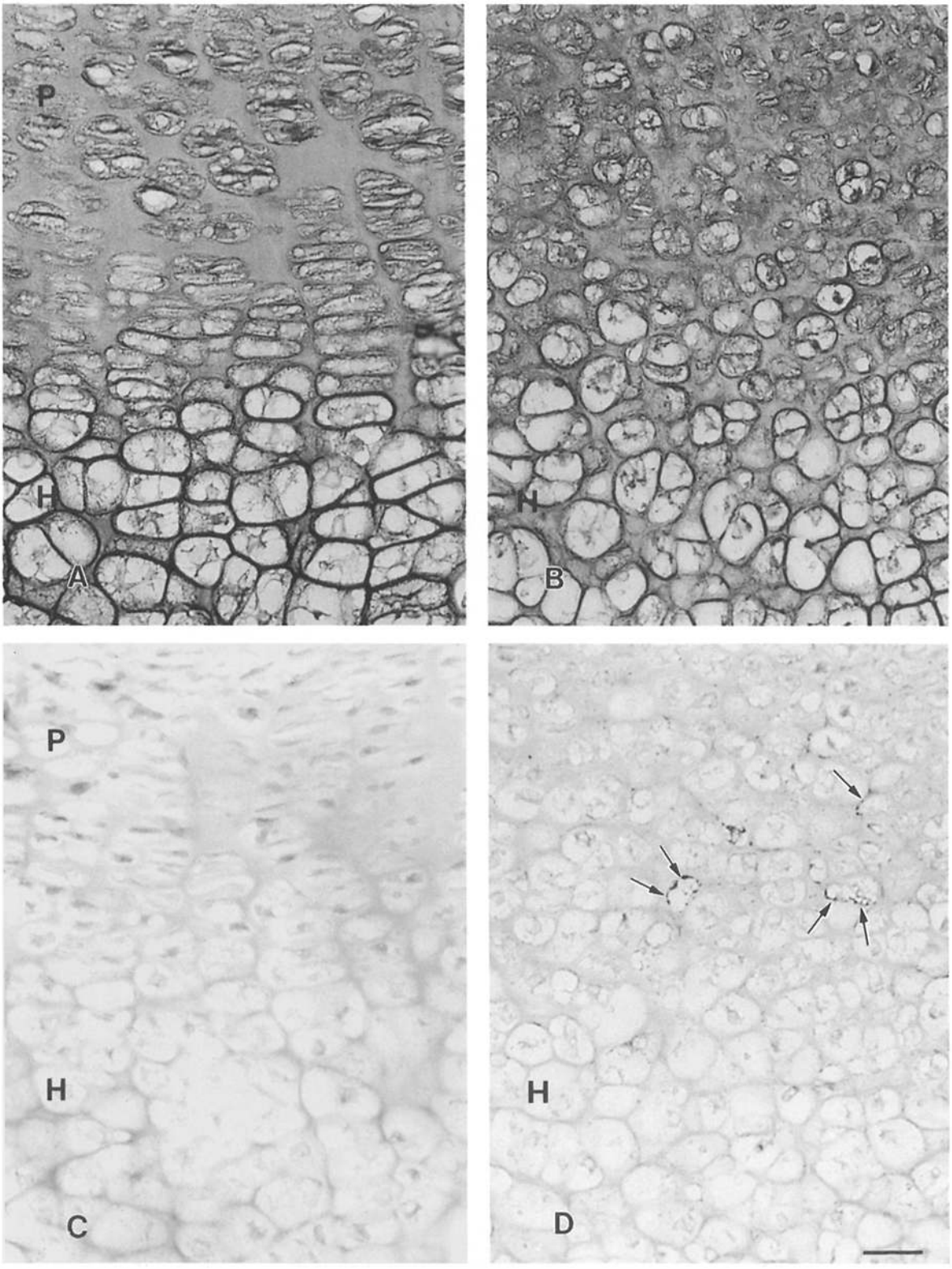

Figure 6. Chondroitin-4-sulfate (*A* and *B*) and cell surface–associated chondroitin sulfate (*C* and *D*) localization as determined by antibodies 2-B-6 and CS-56, respectively, in epiphyses of normal (*A* and *C*) and mutant (*B* and *D*) litter mates. Immunolocalization of chondroitin-4-sulfate displayed uniform reactivity throughout the cartilage matrix of both wild-type and mutant epiphyses. Immunoreactivity to cell surface–associated chondroitin sulfate (*arrows*) was demonstrated on NHC in the mutant epiphysis (*D*) while no staining was evident in the normal hypertrophic zone (*C*). Specimens were counterstained with methyl green. *P*, proliferative zone; *H*, hypertrophic zone. Bar: (*A–D*) 15 μm.

they contained distended cisternae of rough endoplasmic reticulum, a moderately well developed Golgi apparatus, and secretory vesicles (Fig. 4 *F*). In contrast, hypertrophic chondrocytes were large with few organelles. An unusual but characteristic finding in the PTHrP-depleted mice was the presence of large amounts of dispersed glycogen granules in the hypertrophic chondrocytes and large dense masses of glycogen in the cytoplasm of the non-hypertrophic chondrocytes (Figs. 4 *F* and 7 *B*).

The distribution of type II collagen in cartilage matrix of PTHrP-depleted mice was examined using immunofluorescent confocal microscopy. Intense immunoreactivity for type II collagen was observed throughout the cartilage matrix in PTHrP-normal mice (Fig. 5, *A* and *C*). In contrast, staining for type II collagen was very weak in the mutant specimens (Fig. 5, *B* and *D*). However, the non-hypertrophic cells in the hypertrophic zone stained intensely for type II collagen, consistent with their capacity for active protein synthesis as indicated by [^{3}H]proline radioautography.

Monoclonal antibodies recognizing matrix-associated chondroitin-sulfate proteoglycan were used to determine the differential distribution of 4-sulfated (2-B-6) and oversulfated (7-D-4) chondroitin sulfate in normal and mutant epiphyseal cartilage. The distribution of chondroitin-4-sulfate

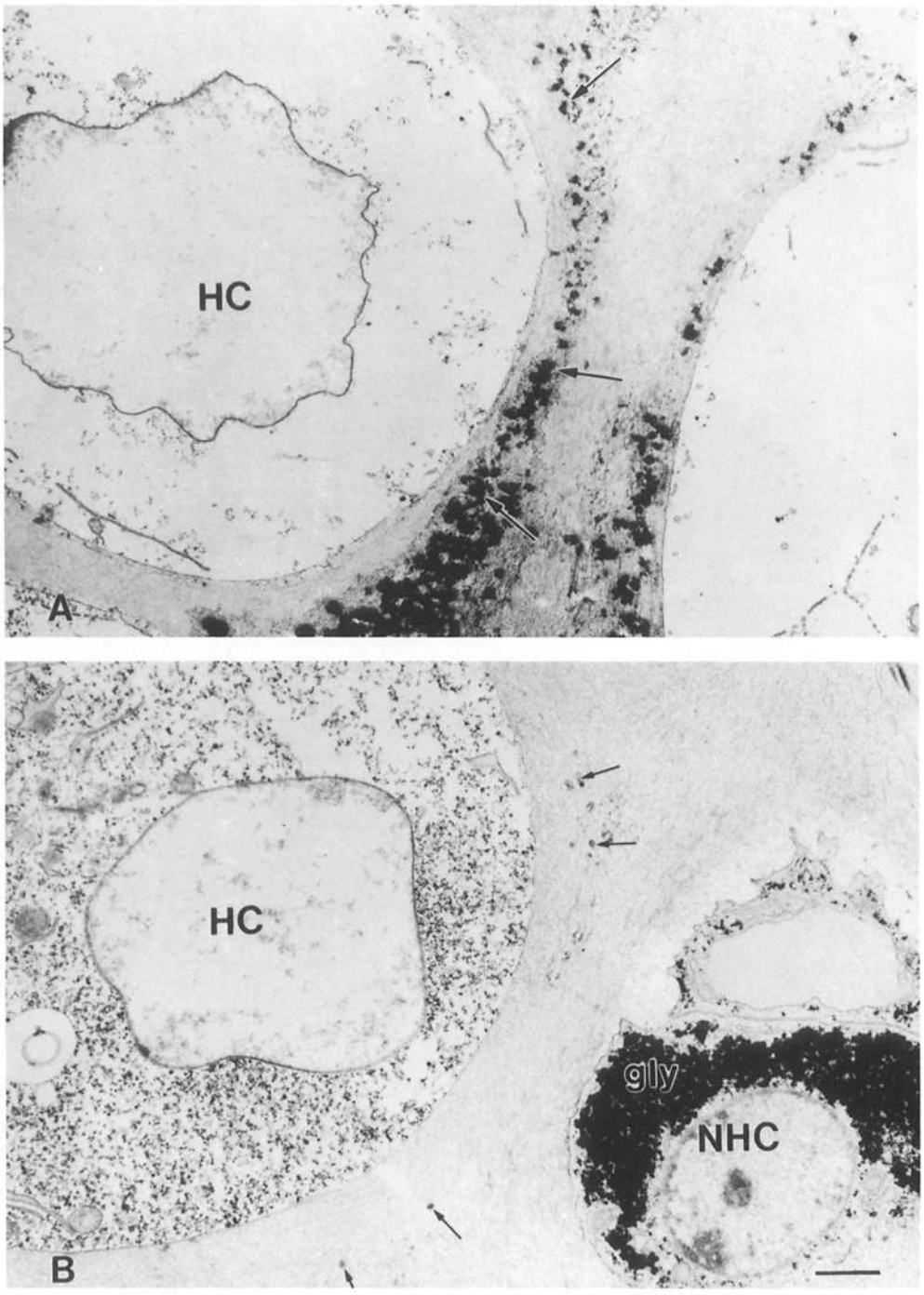

Figure 7. Electron micrographs of the zone of calcifying cartilage of the tibiae of PTHrP-normal (*A*) and PTHrP-depleted (*B*) mice. (*A*) In the normal tibia, the deposition of hydroxyapatite crystals is seen as an accumulation of dense particles (*arrows*) in the longitudinal partitions of cartilage matrix adjacent to the HC. (*B*) In the tibia of PTHrP-depleted mice, there is no accumulation of hydroxyapatite crystals indicating deficient calcification in the cartilage matrix in the region of the NHC, but matrix vesicles (*small arrows*) are present in the matrix adjacent to HC. Non-hypertrophic cells contain massive amounts of cytoplasmic glycogen (*gly*). Bar: (*A* and *B*) 2 μm.

was uniform throughout the extracellular cartilage matrix in all zones of the epiphyses of both normal and homozygous mice (Fig. 6, *A* and *B*). A similar immunohistochemical distribution was observed with antibody 7-D-4 (data not shown).

In constrast, cell membrane–associated chondroitin sulfate, as detected by antibody CS-56, showed altered distribution in the mutant epiphysis. In both normal and mutant specimens, immunoreactivity to CS-56 was associated with cells in the periosteum and articular surface as well as with resting chondrocytes in close proximity to the articular surface (data not shown). However, differences in staining were evident in the mutant hypertrophic zone when compared to its normal counterpart. In the mutant, immunoreactivity was present and was distinctly associated with the cell surface of the non-hypertrophic chondrocytes clustered in the hypertrophic zone (Fig. 6 *D*). No staining with this antibody was detected in the hypertrophic zone of the PTHrP-normal mice (Fig. 6 *C*).

In the zone of calcifying cartilage in PTHrP-normal mice, calcification, in the form of electron dense hydroxyapatite crystals, was uniformly distributed in the longitudinal intercolumnar septae of cartilage matrix between hypertrophic chondrocytes (Fig. 7 *A*). In the PTHrP-depleted mice, calcification occurred unevenly with hydroxyapatite crystals deposited in the vicinity of hypertrophic chondrocytes, but not adjacent to non-hypertrophic cells located in this zone. Matrix vesicles, implicated in the mechanism of initial

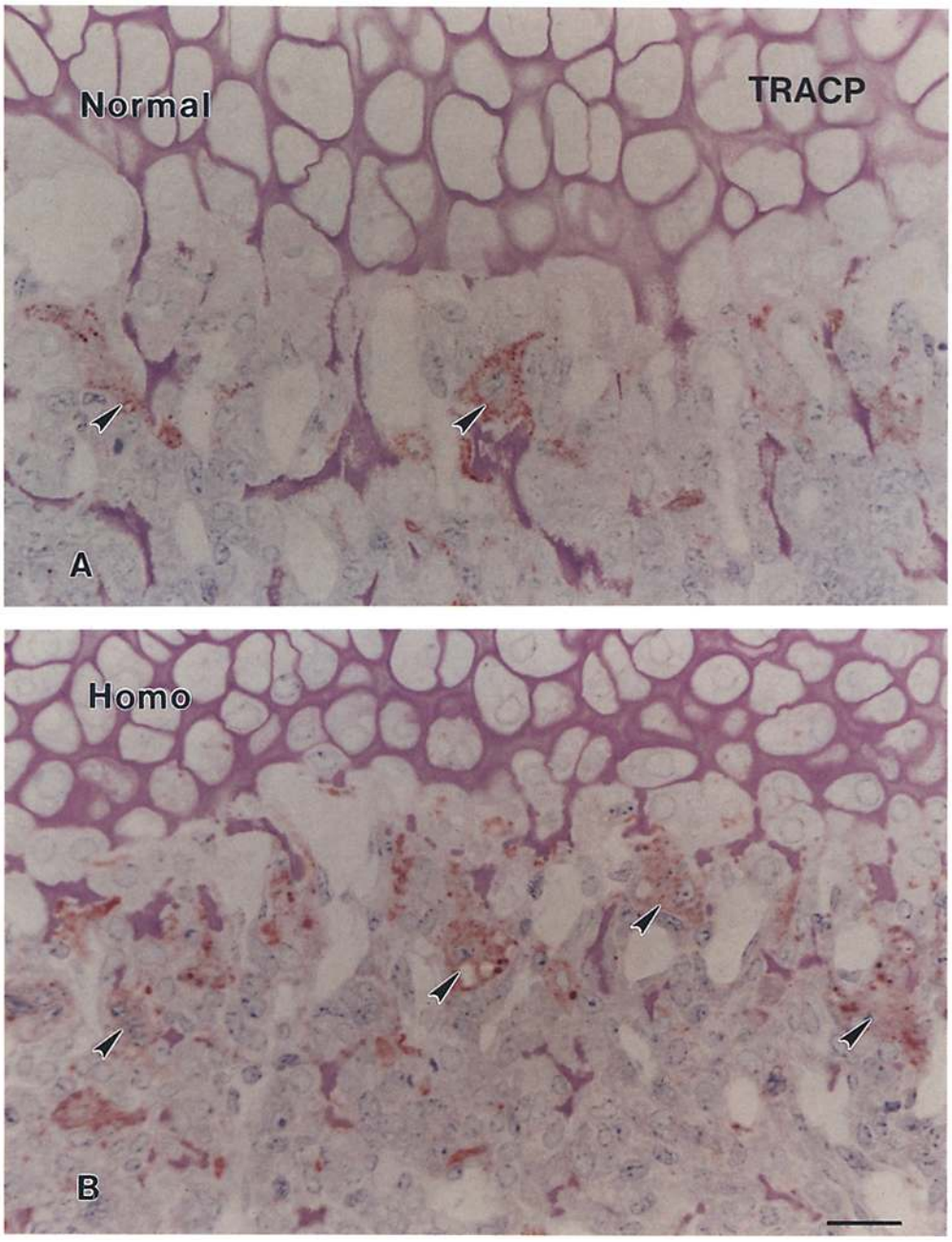

Figure 8. Photomicrographs of the metaphyses of the tibiae of PTHrP-normal (*A*) and PTHrP-depleted (*B*) mice demonstrating TRACPase activity. (*A*) In the PTHrP-normal tibia, TRACPase-positive cells (*arrowheads*) are uniformly distributed in the bone tissue close to the zone of vascular invasion. (*B*) In the tibiae of PTHrP-depleted mice, numerous TRACPase-positive multinucleated cells (*arrowheads*) accumulated close to the epiphysis in contact with the cartilage remnants Bar: (*A* and *B*) 22 μm.

calcification in the zone of calcifying cartilage, were present near hypertrophic chondrocytes, but were not seen near nonhypertrophic cells (Fig. 7 *B*).

Alterations in the Metaphyses of PTHrP-depleted Mice

In the metaphyses of PTHrP-normal mice, the longitudinal cartilage septae between chondrocyte columns became calcified and formed the scaffold for bone deposition forming mixed spicules (Fig. 4 *A*) that paralleled the longitudinal axis of the bone. Spicules in the central portion of the epiphyseal plate were largely resorbed in the metaphysis, but those at the periphery of the plate became incorporated in the metaphyseal wall and formed the fixed point from which bone elongation proceeds. In PTHrP-depleted mice, the cartilage septae in the zone of vascular invasion were few in number, irregularly distributed, and distorted. There were fewer instances of invasion of blood vessels into empty lacunae (Fig. 4 *B* compared to 4 *A*) and many undifferentiated connective tissue and marrow cells aggregated in this zone. These included many TRACPase-positive multinucleated osteoclasts in contact with cartilage remnants (Fig. 8). As a consequence of distorted cartilage scaffolds, there were no longitudinal mixed spicules.

In the PTHrP-normal mice, the calcified cartilage cores were larger than the amounts of bone formed (Fig. 9 *A*), but in the PTHrP-depleted mice, the calcified cartilage remnants were small and irregular while the bone seams were wider relative to the cartilage remnants (Fig. 9 *B*). The distribution of osteocalcin immunoreactivity revealed, in both cases, the unreactive cores of calcified cartilage outlined by a heavily stained band of immunoreactivity, corresponding in position to the lamina limitans (McKee et al., 1993), followed by the less intensely reactive bone (Fig. 9, *A* and *B*). Quantitative radioautography after injection of [^{3}H]proline showed no statistically significant difference in labeling per osteoblast and adjacent matrix over the surface of mixed spicules (data not shown). TRACPase-positive multinucleated osteoclasts were more numerous in whole longitudinal tibial sections of homozygous than in wild-type mice, although no significant differences where seen in the number of TRACPase-positive mononuclear cells (Table I).

No morphological differences were observed in the osteoblasts lining the mixed spicules of PTHrP-normal and PTHrP-depleted mice. In addition, cells with long cytoplasmic processes, presumably of the osteoblastic lineage, were located between the vascular endothelium and bone-lining layer of fully differentiated osteoblasts in both mutant and wild-type specimens. However, in the mutant, these cells contained much larger cytoplasmic accumulations of glycogen than did similar cells in PTHrP-normal bone (Fig. 10 *B* compared to 10 *A*).

Discussion

The present study demonstrates that PTHrP-depleted homozygous fetuses carrying a null mutation in the PTHrP gene have profound abnormalities in the epiphyseal growth plate resulting in abnormal endochondral bone formation. The epiphyseal dysgenesis observed is likely to result, at least in part, from the failure of resting and transitional chondrocytes at the junction of proliferative and hypertrophic zones to produce PTHrP.

The reduced size of the mutant PTHrP-depleted epiphyseal growth plate appears to be due to diminished numbers

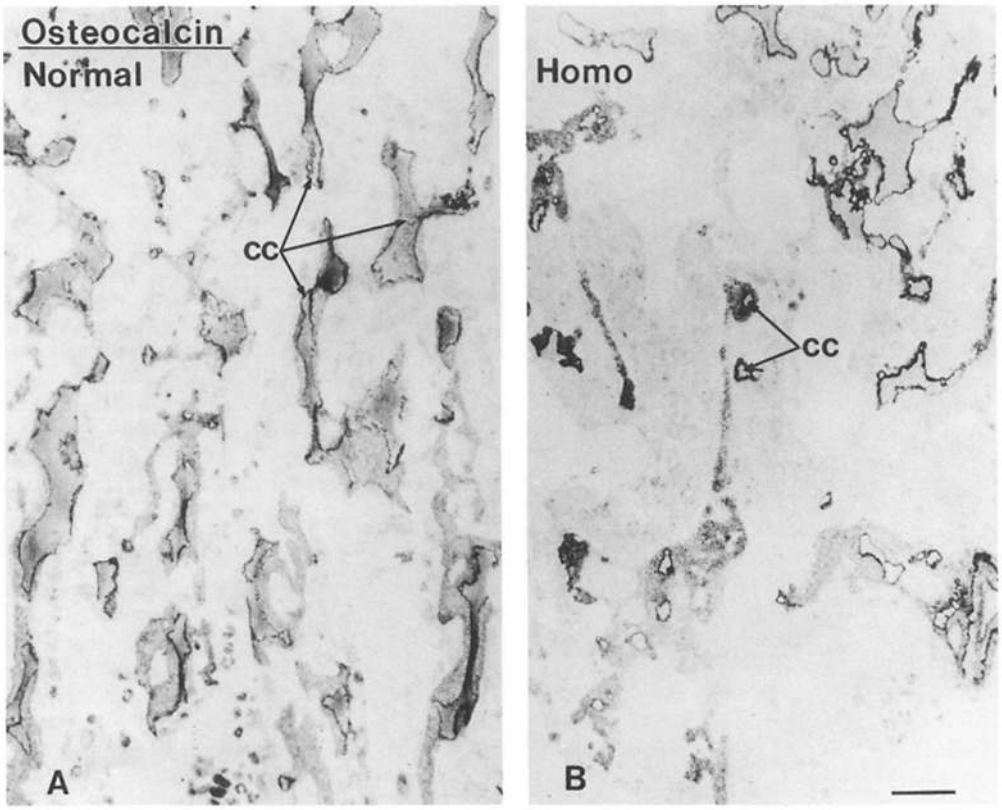

Figure 9. Photomicrographs of the zone of mixed spicules of the tibiae of PTHrP-normal (*A*) and PTHrP-depleted (*B*) mice demonstrating immunoreactivity for osteocalcin. (*A*) In the normal tibia, osteocalcin immunoreactivity is seen as a black line, the lamina limitans, outlining the calcified cartilage cores (*cc*), and over the bone matrix deposited along the cartilage remnants. Cartilage remnants are distributed parallel to the longitudinal axis of the tibia. (*B*) In the tibia of the PTHrP-depleted mouse, the small cores of cartilage remnants (*cc*) are irregularly distributed and surrounded by irregularly shaped large areas of bone immunoreactive for osteocalcin. Bar: (*A* and *B*) 35 μm.

of chondrocytes and this was collaborated by the reduced [^{3}H]thymidine-labeling index. PTH has been reported to exert a mitogenic effect in vitro on embryonic chondrocytes (Koike et al., 1990) and PTHrP may be the endogenous ligand in vivo which plays a similar role through its interaction with the common PTH/PTHrP receptor (Jüppner et al., 1991). Chondrocytes in the resting and proliferative zones of mutant mice were mitotically dysfunctional as well as markedly less active in production of the cartilage-specific type II collagen. Transgenic mice harboring a deletion in proα1(II) collagen also develop chondrodysplasia (Metsäranta et al., 1992), suggesting that the reduction in type II collagen occurring as a consequence of PTHrP deficiency may be contributing to the development of the mutant phenotype.

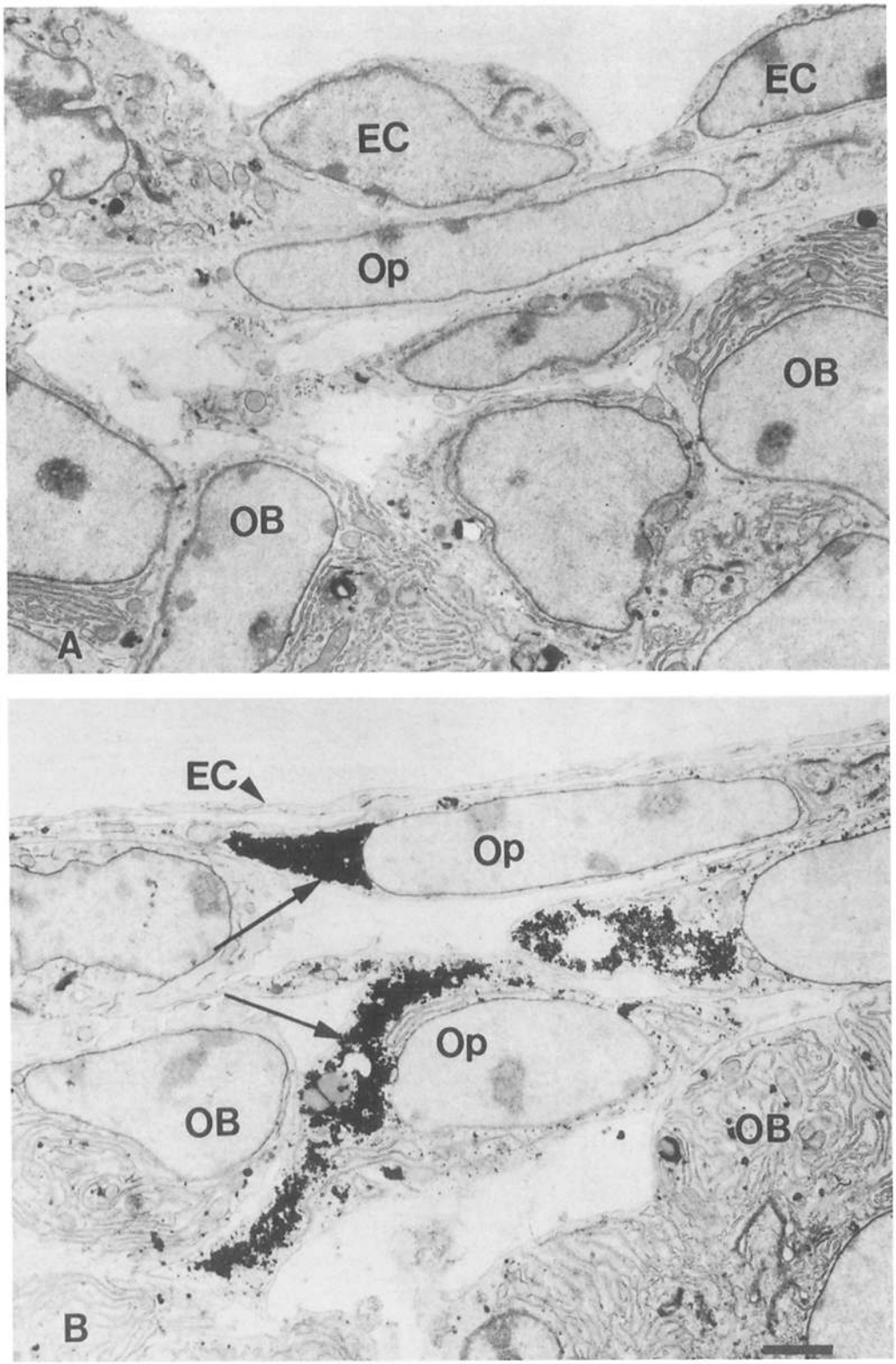

Figure 10. Electron micrographs of the intertrabecular region of the tibial metaphyses of PTHrP-normal (*A*) and PTHrP-depleted (*B*) mice demonstrating presumptive osteoprogenitor (*Op*) cells between endothelial cells (*EC*) and mature osteoblasts (*OB*). These progenitor cells in the PTHrP-normal tibia display prominent Golgi apparatus, mitochondria, and several parallel cisternae of rough endoplasmic reticulum. Dense glycogen granules are seen dispersed in the cytoplasm. (*B*) In the tibiae of PTHrP-depleted mice, massive accumulations of glycogen granules (*arrows*) are observed in this cell type. Bar: (*A* and *B*) 3 μm.

In the mutant epiphysis, the orderly transition from proliferative to hypertrophic chondrocytes is clearly altered. Clusters of non-hypertrophic cells persist in the hypertrophic zone and have characteristics of resting and proliferative chondrocytes, such as the capacity to synthesize DNA, produce type II collagen, and express cell membrane–associated chondroitin sulfate. However, they also have some characteristics of hypertrophic chondrocytes, particularly ALPase activity. Hypertrophic chondrocytes in this zone appear capable of mediating the calcification of the adjacent matrix. However, unlike their normal counterpart, they retain cytoplasmic glycogen granules. Therefore, the orderly process of cell differentiation is markedly perturbed in this zone. This synchronous differentiation process may normally be regulated by PTHrP produced by transitional cells at the junction between proliferative and hypertrophic zones. The recently cloned PTH/PTHrP receptor has also been localized to this region (Lee et al., 1993). We conclude that this altered differentiation process is a consequence of PTHrP deficiency.

Recently, two other putative modulators of cartilage and bone development have been genetically altered in mice by homologous recombination (Shull et al., 1992; Kulkarni et al., 1993; Liu et al., 1993; Baker et al., 1993). Thus, deletion of TGFβ1, a factor reported to be produced in chondrocytes (Rosier et al., 1989; Thorp et al., 1992) and which can promote chondrogenesis after exogenous administration (Noda and Camilliere, 1989; Joyce et al., 1990), resulted in no dramatic phenotypic abnormalities in cartilage and bone (Shull et al., 1992; Kulkarni et al., 1993). On the other hand, mutant mice carrying a null mutation of IGF-1 and type 1 IGF receptor did demonstrate a retarded growth rate associated with delayed bone development (Liu et al., 1993; Baker et al., 1993). However, the phenotypic expression of these mutations was much less severe than the abnormalities in the growth plate and in endochondral bone formation observed in mice with an ablated PTHrP gene. Consequently, PTHrP appears to play a more central role in normal chondrocyte growth and differentiation than either IGF-1 or TGFβ1.

This role of PTHrP as a modulator of the chondrocytic differentiation program is also evident in the zone of vascular invasion. Although it has been postulated that hypertrophic chondrocytes differentiate into osteoblasts in vitro (Strauss et al., 1990; Cancedda et al., 1992), it is more generally accepted that hypertrophic chondrocytes normally die after the formation of calcified cartilage matrix. Yet, in PTHrP-depleted mice, non-hypertrophic chondrocytes persist up to the metaphyseal surface of the epiphyseal cartilage (Fig. 4 *B*). Consequently, the orderly program of cell death normally occurring in the metaphyseal region is clearly altered in the absence of PTHrP.

The number of osteoclasts appears to increase in the metaphyses of PTHrP-depleted mice. It remains to be determined whether this is due to an absence of the carboxyl-domain (107-111) of PTHrP which some studies (Fenton et al., 1991*a*,*b*; 1993) but not others (Sone et al., 1992) have reported to exhibit "osteostatic" properties. Nevertheless, enhanced resorption of cartilage remnants, coupled with reduced production of a scaffold of calcified cartilage, may contribute to defective mixed spicules that do not sustain bone elongation.

As with chondrocytes, particularly non-hypertrophic chondrocytes observed in the hypertrophic zone, putative osteoblastic progenitor cells in homozygous mice contain massive accumulations of glycogen granules in their cytoplasm. These cells have previously been reported to harbor both PTH receptors (Rouleau et al., 1988; 1990) and EGF receptors (Martineau-Doizé et al., 1988), presumed to be characteristics of preosteoblastic cells (Scott, 1967). Consequently, part of the defect in the PTHrP-depleted state may extend to an earlier stage of mesenchymal cell development where a common precursor to both lineages may be dysregulated.

In conclusion, these studies indicate that the absence of PTHrP production alters the temporal and spatial sequence of chondrocyte development and subsequent endochondral bone formation which is necessary for normal bone elongation. This dysfunction appears, in the first instance, to be due to the central in vivo role of PTHrP in the growth and differentiation of chondrocytes.

We would like to thank K. Dickson, S. Bujold, and M. Cheung, Department of Anatomy and Cell Biology, and Dr. A. Robin Poole, Shriners Hospital for Crippled Children, for their assistance with aspects of this work. We express our sincere appreciation to Dr. Hidehiro Ozawa of Niigata University, Japan, for his technical support. We also thank R. Waghmare, M. Sebag, J. Marshal, K. Patel, and D. Allen for their assistance with the preparation of the manuscript.

This work was supported by Medical Research Council of Canada grants (to A. C. Karaplis, H. Warshawsky and D. Goltzman) and by a grant (to D. Goltzman) from the National Cancer Institute of Canada. N. Amizuka and J. E. Henderson are recipients of fellowships from the Royal Victoria Hospital Research Institute and the Medical Research Council of Canada, respectively.

Received for publication 3 January 1994 and in revised form 23 May 1994.

References

Amizuka, N., and H. Ozawa. 1992. Intracellular localization and translocation of 1α,25-dihydroxyvitamin D_3 receptor on osteoblasts. *Arch. Histol. Cytol.* 55:77–88.

Avnur, Z., and B. Geiger. 1984. Immunocytochemical localization of native chondroitin-sulfate in tissues and cultured cells using specific monoclonal antibody. *Cell.* 38:811–822.

Baker, J., J.-P. Liu, E. J. Robertson, and A. Efstratiadis. 1993. Role of insulin-like growth factors in embryonic and postnatal growth. *Cell.* 75:73–82.

Burstone, M. S. 1958. Histochemical demonstration of acid phosphatase with naphtol AS-phosphates. *J. Nat. Cancer Inst.* 21:523–539.

Burtis, W. J., T. Wu, C. Bunch, J. J. Wysolmerski, K. L. Isogna, E. C. Weir, A. E. Broadus, and A. F. Stewart. 1987. Identification of a novel 17,000-dalton parathyroid hormone-like adenylate cyclase-stimulating protein from a tumor associated with humoral hypèrcalcemia of malignancy. *J. Biol. Chem.* 161:7151–7156.

Byers, S., B. Caterson, J. J. Hopwood, and B. C. Foster. 1992. Immunolocation analysis of glycosaminoglycans in the human growth plate. *J. Histochem. Cytochem.* 40:275–282.

Cancedda, F. D., C. Gentili, P. Manduca, and R. Cancedda. 1992. Hypertrophic chondrocytes undergo further differentiation in culture. *J. Cell Biol.* 117:427–435.

Fenton, A. J., B. E. Kemp, R. G. Hammonds Jr., K. Mitchelhill, J. M. Moseley, T. J. Martin, and G. C. Nicholson. 1991*a*. A potent inhibitor of osteoclastic bone resorption with a highly conserved pentapeptide region of parathyroid hormone-related protein; PTHrP [107-111]. *Endrocrinology.* 129:3424–3426.

Fenton, A. J., B. E. Kemp, G. N. Kent, J. M. Moseley, M. H. Zheng, D. J. Rowe, J. M. Britto, T. J. Martin, and G. C. Nicholson. 1991*b*. A carboxyl-terminal peptide from the parathyroid hormone-related protein inhibits bone resorption by osteoclasts. *Endocrinology.* 129:1762–1768.

Fenton, A. J., T. J. Martin, and G. C. Nicholson. 1993. Long-term culture of disaggregated rat osteoclasts: inhibition of bone resorption and reduction of osteoclast-like cell number by calcitonin and PTHrP [107-111]. *J. Cell Physiol.* 155:1–7.

Henderson, J. E., C. Shustik, R. Kremer, S. A. Rabbani, G. N. Hendy, and D. Goltzman. 1990. Circulating concentration of parathyroid hormone-like peptide in malignancy and hyperparathyroidism. *J. Bone Miner. Res.*

5:105–113.

Horiuchi, N., M. P. Caulfield, J. E. Fisher, M. E. Goldman, G. R. McKee, J. E. Reagan, J. J. Levy, R. F. Nutt, S. B. Rodan, T. L. Schofield, et al. 1987. Similarity of synthetic peptide from human tumor to parathyroid hormone *in vivo* and *in vitro*. *Science (Wash. DC)*. 238:1566–1568.

Joyce, M. E., A. B. Roberts, M. B. Sporn, and M. E. Bolander. 1990. Transforming growth factor-β and the initiation of chondrogenesis and osteogenesis in the rat femur. *J. Cell Biol.* 110:2195–2207.

Jüppner, H., A.-B. Abou-Samra, M. Freeman, X. F. Kong, E. Schipani, J. Richards, L. F. Kolakowski Jr., J. Hock, J. T. Potts, Jr., H. M. Kronenberg, and G. V. Segre. 1991. A G protein-linked receptor for parathyroid hormone and parathyroid hormone-related peptide. *Science (Wash. DC)*. 254:1024–1026.

Kaiser, S. M., P. Laneuville, S. M. Bernier, J. S. Rhim, R. Kremer, and D. Goltzman. 1992. Enhanced growth of a human keratinocyte cell line induced by antisense RNA for parathyroid hormone-related peptide. *J. Biol. Chem.* 267:13623–13628.

Kaiser, S. M., M. Sebag, J. S. Rhim, R. Kremer, and D. Goltzman. 1994. Antisense-mediated inhibition of parathyroid hormone-related peptide (PTHrP) production in a keratinocyte cell line impedes differentiation. *Mol. Endocrinol.* 8:139–147.

Karaplis, A. C., A. Luz, J. Glowacki, R. T. Bronson, V. L. J. Tybulewicz, H. M. Kronenberg, and R. C. Mulligan. 1994. Lethal skeletal dysplasia from targeted disruption of the parathyroid hormone-related peptide (PTHrP) gene. *Genes Dev.* 8:277–289.

Kemp, B. E., J. M. Moseley, C. P. Rodda, P. R. Ebeling, R. E. H. Wettenhall, D. Stapleton, N. Diefenbach-Jagger, F. Ure, V. P. Michelangeli, H. A. Simmons, et al. 1987. Parathyroid hormone-related protein of malignancy: active synthetic fragments. *Science (Wash. DC)*. 238:1568–1570.

Koike, T., M. Iwamoto, A. Shimazu, K. Nakashima, F. Suzuki, and Y. Kato. 1990. Potent mitogenic effects of parathyroid hormone (PTH) on embryonic chick and rabbit chondrocytes: different effects of age on growth, proteoglycan, and cyclic AMP responses on chondrocytes to PTH. *J. Clin. Invest.* 85:626–631.

Kulkarni, A. B., C.-H. Huh, D. Becker, A. Geiser, M. Lyght, K. C. Flanders, A. B. Roberts, M. B. Sporn, J. M. Ward, and S. Karlsson. 1993. Transforming growth factor-β1 null mutation in mice causes excessive inflammatory response and early death. *Proc. Natl. Acad. Sci. USA*. 90:770–774.

Kramer, S., F. H. Reynolds Jr., M. Castillo, D. M. Valenzuela, M. Thorikay, and J. M. Sorvillo. 1991. Immunological identification and distribution of parathyroid hormone-related protein polypeptides in normal and malignant tissues. *Endocrinology*. 128:1927–1937.

Lee, K., J. D. Deeds, A. T. Bond, H. Jüppner, A.-B. Abou-Samra, and G. V. Segre. 1993. In situ hybridization of PTH/PTHrP receptor mRNA in the bone of fetal and young rats. *Bone*. 14:341–345.

Liu J.-P., J. Baker, A. S. Perkins, E. J. Robertson, and A. Efstratiadis. 1993. Mice carrying null mutations of the genes encoding insulin growth factor 1 (igf-1) and type 1 IGF receptor (igf1r). *Cell*. 75:59–72.

Martineau-Doizé, B., W. H. Lai, H. Warshawsky, and J. J. M. Bergeron. 1988. *In vivo* demonstration of cell types that harbour epidermal growth factor receptors. *Endocrinology*. 123:841–858.

McKee, M. D., M. C. Farach-Carson, W. T. Butler, P. V. Hauschka, and A. Nanci. 1993. Ultrastructural immunolocalization of noncollagenous (osteopontin and osteocalcin) and plasma (albumin and αHS-glycoprotein) proteins in rat bone. *J. Bone Miner. Res.* 8:485–496.

Merendino, J. J., Jr., K. L. Isogna, L. M. Milstone, A. E. Broadus, and A. F. Stewart. 1986. A parathyroid hormone-like protein from cultured human keratinocytes. *Science (Wash. DC)*. 231:388–390.

Metsäranta, M., S. Garafarlo, G. Decker, M. Rintala, B. de Crombrugghe, and E. Vuorio. 1992. Chondrodysplasia in transgenic mice harbouring a 15-amino acid deletion in the triple helical domain of pro-α1(II) collagen chain. *J. Cell Biol.* 118:203–212.

Noda, M., and J. J. Camillier. 1989. *In vivo* stimulation of bone formation by transforming growth factor-beta. *Endocrinology*. 124:2991–2994.

Oguro, I., and H. Ozawa. 1989. Cytochemical studies of the cellular events sequence in bone remodeling. *J. Bone Metab.* 7:30–36.

Rabbani, S. A., J. Mitchell, D. R. Roy, G. N. Hendy, and D. Goltzman. 1988. Influence of the amino-terminus on *in vitro* and *in vivo* biological activity of synthetic parathyroid hormone-like peptides of malignancy. *Endocrinology*. 123:2709–2716.

Rodan, S. B., K. L. Isogna, A. M.-G. Vignery, A. F. Stewart, A. E. Broadus, S. M. D'Souza, and D. R. Bertolini. 1983. Factors associated with humoral hypercalcemia of malignancy stimulate adenylate cyclase in osteoclastic cells. *J. Clin. Invest.* 72:1511–1515.

Rosier, R. N., R. J. O'Keefe, I. D. Craab, and J. E. Puzas. 1989. Transforming growth factor beta: an autocrine regulation of chondrocytes. *Connect. Tissue Res.* 20:295–301.

Rouleau, M. F., J. Mitchell, and D. Goltzman. 1988. *In vivo* distribution of parathyroid hormone receptors in bone: evidence that a predominant osseous target cell is not the mature osteoblast. *Endocrinology*. 123:187–191.

Rouleau, M. F., J. Mitchell, and D. Goltzman. 1990. Characterization of the major parathyroid hormone target cell in the endosteal metaphysis of rat long bones. *J. Bone Miner. Res.* 5:1043–1053.

Scott, B. L. 1967. Thymidine-^{3}H electron microscope radioautography of osteogenic cells in the fetal rat. *J. Cell Biol.* 35:115–126.

Senior, P. V., D. A. Heath, and F. Beck. 1991. Expression of parathyroid hormone-related protein mRNA in the rat before birth: demonstration by hybridization histochemistry. *J. Mol. Endocrinol.* 6:281–290.

Shull, M. M., I. Ormsby, A. B. Kier, S. Pawloski, R. J. Diebold, M. Yin, R. Allen, C. Sidman, G. Proetzel, D. Calvin, et al. 1992. Targeted distribution of the mouse transforming growth factor-β 1 gene results in multifocal inflammatory disease. *Nature (Lond.)*. 359:693–699.

Slot, J. W., and H. J. Geuze. 1985. A new method of preparing gold probes for multiple-labeling cytochemistry. *Eur. J. Cell Biol.* 38:87–93.

Sone, T., H. Kohno, H. Kikuchi, T. Ikeda, R. Kasai, Y. Kikuchi, R. Takeichi, J. Konishi, and C. Shigeno. 1992. Human parathyroid hormone-related peptide-(107-111) does not inhibit bone resorption in neonatal mouse calvariae. *Endocrinology*. 131:2742–2746.

Stolpe, A. van de, M. Karperien, C. W. G. M. Löwik, H. Jüppner, G. V. Segre, A.-B. Abou-Samra, S. W. de Laat, and L. H. K. Defize. 1993. Parathyroid hormone-related peptide as an endogenous inducer of parietal endoderm differentiation. *J. Cell Biol.* 120:235–243.

Strauss, P. G., E. I. Closs, J. Schmidt, and V. Erfle. 1990. Gene expression during osteogenic differentiation in mandibular condyles *in vitro*. *J. Cell Biol.* 110:1369–1378.

Strewler, G. J., P. H. Stern, J. W. Jacob, J. Eveloff, R. F. Klein, S. C. Leung, M. Rosenblatt, and R. A. Nissenson. 1987. Parathyroid hormonelike protein from human renal carcinoma cells: structural and functional homology with parathyroid hormone. *J. Clin. Invest.* 80:1803–1807.

Suva, L. J., G. A. Winslow, R. E. H. Wettenhall, R. G. Hammonds, J. M. Moseley, H. Diefenbach-Jaggar, C. P. Rodda, B. E. Kemp, H. Rodriguez, E. Y. Chen, et al. 1987. A parathyroid hormone-related protein implicated in malignant hypercalcemia: cloning and expression. *Science (Wash. DC)*. 237:893–896.

Thiede, M. A., and G. A. Rodan. 1988. Expression of a calcium-mobilizing parathyroid hormone-related peptide in lactating mammary tissue. *Science (Wash. DC)*. 242:278–280.

Thorp, B. H., I. Anderson, and S. B. Jakowlew. 1992. Transforming growth factor-β1, -β2 and -β3 in cartilage and bone cells during endochondral ossification in the chick. *Development*. 114:907–911.

Warshawsky, H., and G. Moore. 1967. A technique for the fixation and decalcification of rat incisors for electron microscopy. *J. Histochem. Cytochem.* 15:524–549.

Wysolmerski, J. J., A. E. Broadus, J. Zhou, E. Fuchs, L. M. Milstone, and W. M. Philbrick. 1994. Overexpression of parathyroid hormone-related peptide in the skin of transgenic mice interferes with hair follicle development. *Proc. Natl. Acad. Sci. USA*. 91:1133–1137.